THE ASTROPHYSICAL JOURNAL, **268**:739–752, 1983 May 15

STELLAR WINDS AND MOLECULAR CLOUDS: T TAURI STARS

NURIA CALVET,[1] JORGE CANTÓ,[2] AND L. F. RODRÍGUEZ[2]
Received 1982 February 8; accepted 1982 September 17

ABSTRACT

We searched for high-velocity molecular gas in the environment of 12 T Tauri stars associated with optical nebulosities. The molecular gas associated with T Tau and HL and HZ Tau clearly showed carbon monoxide line wings extending at least over ~ 15 km s^{-1}. HL and XZ Tau are located in the molecular cloud L1551, where an independent outflow powered by an infrared source has been reported. The existence of two separate centers of gas outflow in L1551 suggests that the phenomenon is common. The rate of momentum being injected by stars as T Tau and HL and XZ Tau into their molecular surroundings is large, $\gtrsim 10^{-6}$ $M_\odot$ km s^{-1} yr^{-1}. These rates are higher than those expected from the radiative momentum rate of the stars alone, but comparable with those derived from optical observations of T Tau winds.

Subject headings: interstellar: molecules — line profiles — radio sources: lines — stars: mass loss — stars: pre-main-sequence — stars: winds

I. INTRODUCTION

The T Tauri stars are generally believed to be stars of low mass ($\lesssim 2$ $M_\odot$) and luminosity ($\lesssim 10$ $L_\odot$) in their pre–main-sequence convective track (Cohen and Kuhi 1979). They have ages usually less than 10^6 yr (Rydgren, Strom, and Strom 1976) and, correspondingly, are still associated physically with their parent molecular cloud (Herbig 1977). The presence of a T Tauri star is expected to affect the associated molecular cloud in several detectable ways. The stellar radiation will heat the dust in the cloud, and via collisions the dust will heat the gas. The dust will radiate detectable amounts of infrared photons (Beichman and Harris 1981; Fridlund *et al.* 1982). Also the heated gas can be detected by means of the carbon monoxide rotational transitions. For a molecular cloud with a density of $n_{H_2} \approx 3 \times 10^3$ cm^{-3}, the ambient cosmic rays will provide a heating rate of $\Gamma_{cr} \approx 1.9 \times 10^{-24}$ ergs cm^{-3} s^{-1}, maintaining the gas at a kinetic temperature of $T_K \simeq 8$ K (Goldsmith and Langer 1978). The beamwidth of the Kitt Peak 11 m radiotelescope at the frequency of the CO $J = 1 \rightarrow 0$ rotational transition is 66″. At the distance of the Taurus molecular complex (160 pc), this means that one is sampling gas at typical distances of (neglecting line-of-sight effects) ~ 0.03 pc from the central stars. A star with a luminosity of 10 $L_\odot$ will heat the dust to a temperature of about 20 K (Loren and Wootten 1978) and dust-gas heat transfer will raise the kinetic temperature of the cloud to $T_K \approx 10$ K (Leung 1975). This implies that the heating due to stellar radiation is likely to be detected in the vicinity of the star. On the other hand, the wind of a T Tauri star is also expected to affect the cloud kinematically. The wind could accelerate molecular gas to radial velocities different from those of the ambient cloud; this velocity-shifted gas could be detectable as wings or bumps in CO spectra with a good signal-to-noise ratio. It is now well known that recently formed OB stars can produce outflows detectable in CO and sometimes in other molecules. Some of the best studied examples are Orion (Zuckerman, Kuiper, and Rodríguez Kuiper 1976; Kwan and Scoville 1976; Solomon, Huguenin, and Scoville 1981) and Cepheus A (Rodríguez, Ho, and Moran 1980; Ho, Moran, and Rodríguez 1982). The detection of an outflow in L1551 (Snell, Loren, and Plambeck 1980) powered by an infrared source identified by Beichman and Harris (1981) as a forming T Tauri star, suggests that visible T Tauri stars could also power gas outflows. The strength of the T Tauri winds will determine if such outflows are detectable.

Roughly, the size R of the region which is expected to be dynamically affected by a wind-producing star with mass loss rate $\dot{M}_\star$ and terminal velocity $V_\star$ immersed in a medium with density n and temperature T, can be estimated assuming pressure equilibrium, that is,

$$\frac{\dot{M}_\star V_\star}{4\pi R^2} \approx nkT,$$

or

$$\left(\frac{R}{\text{pc}}\right) \approx 0.62\left[\left(\frac{\dot{M}_\star}{10^{-7}\,M_\odot\ \text{yr}^{-1}}\right)\left(\frac{V_\star}{100\ \text{km}^{-1}}\right) \times\left(\frac{n}{10^3\ \text{cm}^{-3}}\right)^{-1}\left(\frac{T}{10\ \text{K}}\right)^{-1}\right]^{1/2}.$$

Adopting as typical values for T Tauri stars (as quoted

[1] Centro de Investigación de Astronomía, Mérida, Venezuela.
[2] Instituto de Astronomía, Universidad Nacional Autónoma de México.

in the literature) and the associated cloud those that make the bracketed quantity on the right-hand side equal to unity, a region of about $\leq 25'$ in extent is expected to be affected by the wind of a T Tauri star in the Taurus molecular complex. Theoretical expectations, on the other hand, are not conclusive given considerable uncertainties on the parameters of the winds of T Tauri stars. DeCampli (1981), for instance, suggests that the mass loss rates deduced from the Hα line intensity alone can have an ambiguity of orders of magnitude. He also notes that most T Tauri stars present nearly symmetric line profiles and that in these cases the mass loss rate could be zero. Further knowledge on the parameters of T Tauri winds is needed since they have been proposed to be the source of energy for the Herbig-Haro objects (Schwartz 1978; Cantó 1978; Cantó and Rodríguez 1980), the supporters of turbulence in molecular clouds (Norman and Silk 1980; Franco 1983), and the clearing agent of residual gas in recently formed planetary systems (Elmegreen 1978).

In this paper we study the winds of T Tauri stars indirectly by obtaining radio observations which try to detect the kinematical effects produced by the wind on the associated cloud. We searched for CO wings in the molecular environments of 12 T Tauri stars and four YY Orionis stars.

All the 12 T Tauri stars selected as sources are associated with optical nebulosity. Eight of these stars are in closely associated pairs, typically between 10″ and 30″. We refer to these pairs as single sources: FM and CW Tau, DD and CZ Tau, HL and XZ Tau, and GI and GK Tau. The other four T Tauri stars observed were RY Tau, T Tau, DG Tau, and DO Tau.

Three of these sources, DG Tau, HL and XZ Tau, and DO Tau, have photospheres corresponding to late spectral types or are "continuum" stars (Cohen and Kuhi 1979), and their spectra are characterized by strong emission lines, ultraviolet emission, and infrared excesses. DG Tau has recently shown a very powerful flare in X-rays (Feigelson and DeCampli 1981). These observations suggest a high degree of activity on the surface of these stars. In addition, two of them, DG Tau and HL and HZ Tau, have only upper limits in their soft X-ray emission (Feigelson and DeCampli 1981; Walter and Kuhi 1981), except for the flare event in DG Tau. Since these stars have very large equivalent widths in Hα, they are expected to have massive extended envelopes which absorb the X-ray emission and emit most of the observed Hα (Gahm 1981; Walter and Kuhi 1981). This suggestion and the presence of blueshifted absorption components in Hα with displacements between 80 and 90 km s^{-1} (Herbig 1977) point to the existence of a massive wind around the stars. The close association of these stars with red nebulosities can tentatively be explained also in terms of a strong wind shocking the cloud and producing collisional excitation in it. For these reasons, we expected these sources to have powerful winds. The strengths of these winds are expected to be related to the degree of activity in the surface of the star (and therefore to the level of nonradiative energy production and deposition near the surface).

Other three sources, FM and CW Tau, DD and CZ Tau, and GI and GK Tau also have late-type photospheres, but their emission-line strength is lower than in the previous group, suggesting that the level of activity on their surfaces is also lower. Blueshifted absorption components have been detected in the Hα profile of some of these stars (Herbig 1977), pointing to the existence of velocity fields in an extended envelope. On the other hand, GI Tau, the only one observed in X-rays among these stars, has been detected as a soft X-ray source (Walter and Kuhi 1982). This detection and the low equivalent width in Hα seem to indicate that the mass in the extended envelope around this star is small. The similarity in spectral characteristics of all the stars in this group suggests that their extended envelopes are also thin and their winds less massive than those in the previous group. In addition, these stars are surrounded by reflection nebulosities (as estimated from their colors on Palomar Sky Survey plates), which we take as a further indication that their winds are less powerful.

We also included in our study T Tau and RY Tau. These stars have hotter photospheres and higher luminosities than stars in the previous groups (Cohen and Kuhi 1979) and are associated with bright red nebulosities. In T Tau, the associated nebulosity (Burnham's Nebula) is known to have a spectrum similar to those of the Herbig-Haro objects, indicative of shocked gas (Schwartz 1975; Raymond 1979), and the extended emission region around it presents evidence of gas moving at supersonic speeds (Schwartz 1975; Cantó 1980). We searched for the influence of this strong wind in the molecular surroundings of T Tau, and also in that of RY Tau, a star of similar nature.

Finally, we also observed four YY Orionis-type stars: YY Ori, CE Ori, MM Mon, and MO Mon. Several authors (Walker 1972, 1978; Appenzeller 1977, and references therein) have suggested that these stars are still having infall of material. We considered it important to search for evidence of outflow in some of them. Unfortunately, none of the nine YY Ori stars given by Walker (1972) have an associated nebulosity that could indicate physical association with the parent cloud. Thus, our results on the YY Ori stars have little significance since the stars could have a net outflow but still be far from the projected molecular cloud.

The observations are described in § II, and our results and interpretation are given in § III. Finally, in § IV we summarize our work.

II. OBSERVATIONS

The CO and ^{13}CO observations were made during 1981 March 27–30 using the 11 m radiotelescope of the

TABLE 1

OBSERVED T TAURI STARS

Star	Central Position[a] α (1950)	Central Position[a] δ (1950)	Reference Position α (1950)	Reference Position δ (1950)	Distance[b] (pc)	Luminosity[c] ($L_\odot$)	Spectrum[c]
FM and CW Tau[d] ...	04^h11^m09^s.6	+28°04′23″	04^h10^m00^s.0	+32°00′00″	160	0.5,2.2	M0,K3
DD and CZ Tau[e]	04 15 25.5	+28 09 45	04 10 00.0	+32 00 00	160	1.9,0.9	M1,M1.5
RY Tau	04 18 50.8	+28 19 35	04 10 00.0	+32 00 00	160	17	K1
T Tau	04 19 04.2	+19 25 05	04 24 32.4	+18 07 37	160	28	K1
DG Tau	04 24 00.9	+25 59 36	04 10 00.0	+32 00 00	160	≥ 7.6	C
HL and XZ Tau[f]	04 28 44.4	+18 07 37	04 24 32.4	+18 07 37	160	≥ 4.4, 10.7	C(K7?),M3
GI and GK Tau[g]	04 30 32.3	+24 15 03	04 24 32.4	+18 07 37	160	1.9,3.5	K7,K7
DO Tau	04 35 24.2	+26 04 56	04 10 00.0	+32 00 00	160	3.5	K7–M0
YY Ori	05 32 20.8	−05 59 53	05 24 20.8	−05 59 53	460	2.8	K5
CE Ori	05 33 19.8	−05 03 28	05 33 19.8	−04 03 28	460	0.8	K5
MM Mon	06 38 28.2	+09 55 37	06 46 58.7	+09 29 53	800	5.0	K3
MO Mon	06 38 46.7	+09 29 53	06 46 58.7	+09 29 53	800	5.9	K2

[a] From Herbig and Rao 1972.

[b] Distances were adopted from Kuhi 1964, Herbig 1966, and Walker 1956.

[c] From Cohen and Kuhi 1979.

[d] The position is midway between FM Tau and CW Tau.

[e] The position is that of CZ Tau.

[f] The position is that of HL Tau.

[g] The position is that of GI Tau.

National Radio Astronomy Observatory[3] at Kitt Peak, Arizona. We used the cooled 80–120 GHz mixers with feeds polarized orthogonally. We did not use the Fabry-Pérot image rejection filter, and the data was calibrated using the chopper wheel technique and comparing with standard sources (Ulich and Haas 1976). The system temperature was in the range 1500–2500 K. Each polarization fed one-half of the two filter banks used (100 and 500 kHz). The halves of each filter bank were averaged, resulting in spectra of 128 points and velocity resolutions of 0.26 and 1.30 km s^{-1} at the frequency of the $J = 1 \rightarrow 0$ rotational transition of CO, 115.27120 GHz. The data were taken by position switching every minute against a reference position previously checked to be free of CO emission to a 4 σ level of ~ 0.5 K. All sources, with the exception of FM and CW Tau were observed in CO at a central position and at four other positions displaced 60″ to the N, E, S and W of the central position. FM and CW Tau were observed in a 3×3 grid with elements separated 60″ and centered halfway between FM Tau and CW Tau. In some of the sources, data were taken at several other positions. In particular, we did N-S and E-W cuts of seven points in T Tau and of four points in HL and XZ Tau to obtain information on the approximate extent of the outflows. These points were made at a separation of 60″. The central and reference positions observed are given in Table 1. For some sources in the Taurus region it was necessary to use distant reference positions to avoid detectable CO emission. Monitoring of the 500 kHz data showed that the baselines remained flat. We also observed ^{13}CO at the central position. The CO and ^{13}CO 100 kHz spectra at the central positions are shown in Figure 1. In order to compare the CO and ^{13}CO spectra in velocity space, we deleted three channels at each end of the ^{13}CO spectrum and stretched it to align with the CO spectrum.

[3] The NRAO is operated by Associated Universities, Inc., under contract with the National Science Foundation.

III. RESULTS

Table 2 shows the CO and ^{13}CO observed and derived parameters in the line of sight to the observed stars (corresponding to the spectra shown in Fig. 1). With the exception of CE Ori which is located close to the Orion Nebula, all sources showed CO peak line temperature in the range of $5 \sim 10$ K. This line temperature range implies kinetic temperatures within about $8 \sim 12$ K, as expected from clouds heated mainly by cosmic rays (Goldsmith and Langer 1978) and lacking the presence of a nearby highly luminous star.

First, it is interesting to compare the optical extinctions derived from optical observations of the stars with those derived from the CO data for the line of sight across the cloud. Of the twelve-sources observed, there are 10 with determined optical extinctions (Cohen and Kuhi 1979). It follows from our radio observations that all these sources, with the exception of RY Tau, have A_V (radio) $\geqslant A_V$ (optical). This result suggests that the stars are located in the near side of the molecular cloud or within it and not behind it. RY Tau is located near the

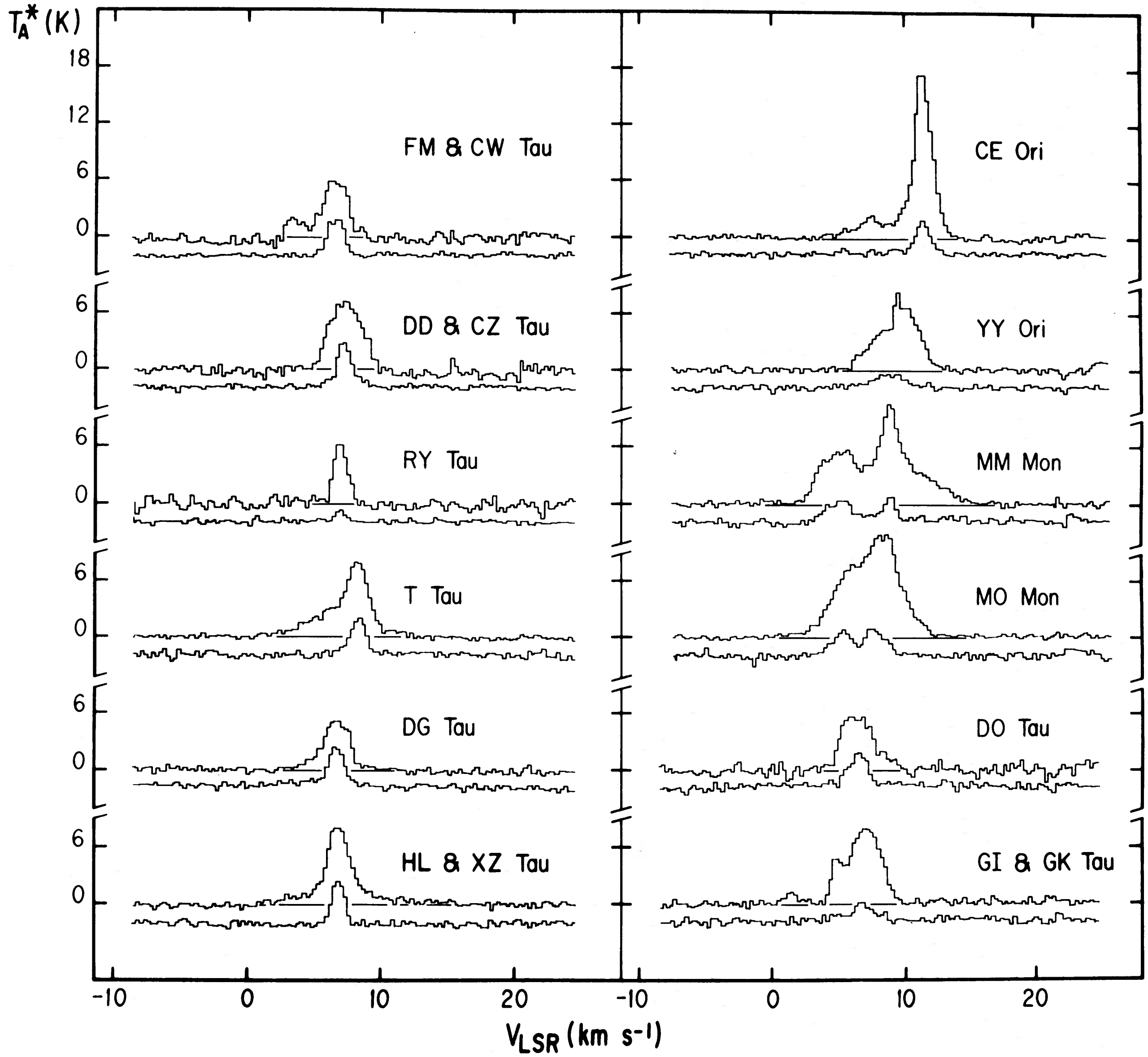

FIG. 1.—$J = 1 \rightarrow 0$ CO and ^{13}CO 100 kHz spectra of the central position of the observed sources. Three channels at each end of the ^{13}CO spectra were deleted and the spectra stretched to align with the CO spectra. The solid line in the CO spectra marks the zero intensity level.

edge of a molecular cloud, and most of its extinction must be circumstellar since the CO data indicate that there is not sufficient interstellar gas in the line of sight to explain the extinction.

Second, we searched for CO wing emission in the spectra using the following criteria: (1) the full width at zero power of the wings should exceed 10 km s^{-1}; (2) the full width at zero power of the wings should be greater than 3 times the full width at half-power of the main line emission; (3) the total emission profile should be relatively simple, that is, lacking multiple components that could be due to line-of-sight clouds; and (4) the wing emission should diminish in intensity as we move a few arc minutes away from the central star. These criteria single out obvious cases of high-velocity mass outflow. However, they could lead to missing low velocity cases of outflow, such as R Mon (Cantó *et al.* 1981), that can only be revealed by a detailed study of the region.

The main observational result of our search is the detection of moderately broad wings in the CO spectra toward T Tau and HL and XZ Tau. These wings are

TABLE 2

OBSERVED AND DERIVED PARAMETERS IN THE LINE OF SIGHT OF T TAURI STARS

	Parameters[a] of ^{12}CO Emission			Parameters[b] of ^{13}CO Emission							
Star	T_{peak} (K)	Δv (km s^{-1})	v_{LSR} (km s^{-1})	T_L (K)	Δv (km s^{-1})	v_{LSR} (km s^{-1})	$N(H_2)$[c] (10^{21} cm^{-2})	A_V[c] (mag)	θ[d] (arcmin)	L[e] (pc)	n_{H_2}[f] (10^3 cm^{-3})
FW and CW Tau ...	5.9	2.1	6.3	4.0	1.4	6.7	4.3	3.4	20	0.93	1.5
DD and CZ Tau	7.1	2.9	7.4	4.6	1.3	7.3	4.6	3.7	18	0.84	1.8
RY Tau	6.2	1.0	6.8	1.1	0.9	7.0	0.5	0.4	6	0.28	0.6
T Tau................	7.8	2.3	8.1	3.7	1.4	8.3	3.4	2.7	12	0.56	2.0
DG Tau	5.1	2.1	6.8	4.1	1.5	6.7	5.6	4.4	10	0.47	3.9
HL and XZ Tau	8.0	2.1	6.6	4.5	1.1	6.8	3.6	2.9	10	0.47	2.5
GI and GK Tau	7.8	2.6	6.8	1.6	2.4	6.7	2.1	1.7	5:	0.23:	3.0:
DO Tau	5.6	2.9	6.0	3.5	1.9	6.4	4.7	3.8	12	0.56	2.7
YY Ori	8.1	2.3	9.7	1.3	3.4	8.9	2.4	1.9	...	...	...
CE Ori	17.1	1.3	11.7	3.3	1.3	11.6	3.3	2.6	...	...	...
MM Mon[g]..........	5.6	3.6	5.8	2.1	2.6	5.2	3.1	2.5	...	...	...
	10.3	2.1	8.9	2.5	1.1	8.9	1.7	1.4	...	...	...
MO Mon[g]..........	7.5	2.9	6.0	2.5	1.7	5.2	2.5	2.0	...	...	...
	10.6	3.9	8.6	2.7	1.9	7.7	3.2	2.6	...	...	...

[a] T_{peak} is the temperature at the peak channel, Δv is the full width at $T_{peak}/2$, and v_{LSR} is the radial velocity of the peak channel with respect to the LSR.

[b] The ^{13}CO parameters were obtained by means of least squares fits to Gaussian profiles. T_L is the line antenna temperature, Δv is the full width at half intensity, and v_{LSR} is the radial velocity of the center of the line with respect to the LSR.

[c] Derived from the formulation of Dickman 1978.

[d] Angular dimension of associated molecular surroundings. For the sources in Orion and Monoceros, we could not assign reliable dimensions.

[e] Physical dimension of associated molecular surroundings.

[f] Derived dividing the column density over the physical dimension.

[g] MM Mon and MO Mon show two distinct spectral components; their parameters are given separately.

similar to those observed in other pre–main-sequence objects (see, for instance, Rodríguez *et al.* 1982) in the sense that their shape can roughly be fitted by a power law of the form $T_A^* \propto v_r^{-\alpha}$, where v_r is the radial velocity with respect to the ambient molecular cloud. For the blue wing of T Tau our best fit gives $\alpha = 2.5$, while for HL and XZ Tau, $\alpha = 1.2$ for the blue wing and $\alpha = 1.4$ for the red wing (although this latter value may have little significance; see below). T Tau also shows a very weak red wing. This goes against the general tendency, which is for sources to show roughly comparable red and blue wings (Rodríguez *et al.* 1982). The line wings in T Tau have also been observed by Knapp *et al.* (1977) and more recently by Edwards and Snell (1981). DG Tau, CE Ori, and MM Mon also show velocity-shifted emission that could be interpreted as wings. However, we did not consider them as unambiguous examples given that the DG Tau wing emission extends over only a few km s^{-1}, and that the spectra from CE Ori and MM Mon are rather complex and the apparent wing emission could well be another CO component along the line of sight since it appears at the other observed positions.

Figures 2 and 3 show velocity versus position contour maps of the corrected antenna temperature for N-S and E-W cuts along the positions of T Tau and HL Tau. The antenna temperature peaks at the position of T Tau, suggesting that in fact at least for this object, there is a detectable heating effect. In HL and XZ Tau the red outflow is contaminated by the red component of the large scale outflow detected by Snell, Loren and Plambeck (1980). Thus, the slope of the red wing in HL and XZ Tau is an unreliable value. Nevertheless, it can be inferred from Figure 3 that the outflow detected in the HL and XZ Tau region is independent from that centered on L1551 IR (Beichman and Harris 1981), since the uncontaminated blueshifted component peaks within 30″ of HL and XZ Tau. Although our angular resolution does not allow to distinguish if the center of the outflow is located in HL Tau or in XZ Tau, other results point toward HL Tau as the source of energy. From spectrophotometric and spectropolarimetric observations, Cohen and Schmidt (1983) have identified HL Tau as the exciting/illuminating star of HH 30. This result favors HL Tau as the dominant source of wind in the region.

T Tau and HL and XZ Tau are in our group of stars with active surfaces and, as expected, showed CO wings, indicating the presence of strong stellar winds. Furthermore, none of the stars in our second group (less active surfaces) showed evidence of wings. However, since there was not a one-to-one correlation between stellar

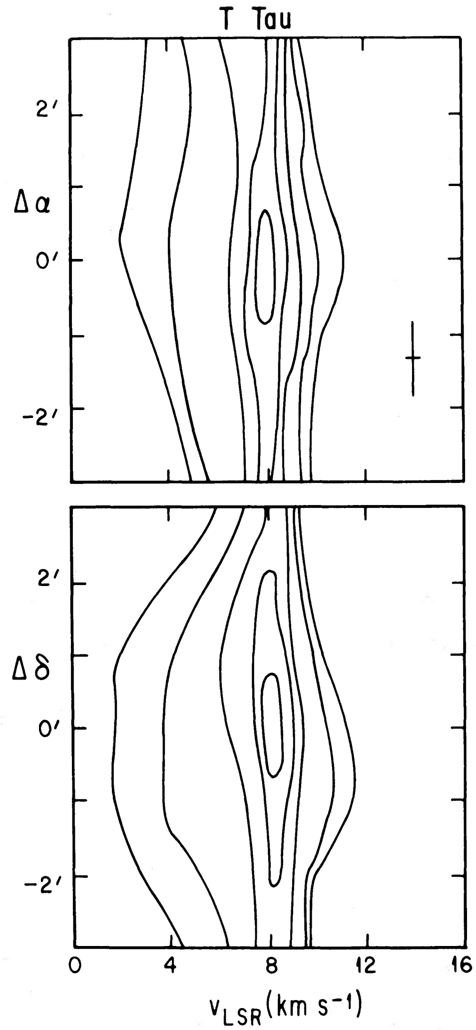

FIG. 2.—Contour maps of the corrected antenna temperature for N-S and E-W cuts along the position of T Tau. Contour values are 0.5, 1.0, 3.0, 5.0, and 7.0 K. Bars indicate angular and velocity resolutions.

characteristics and the presence of CO wings, we can only conclude that our results are consistent with the notion that the most active stars have strong winds. One has to remember that both strong stellar winds and abundant surrounding gas are required to produce detectable CO wings. An example of an object having the first condition but not the second could be RY Tau, which has an active surface but seems to lack abundant associated gas.

In what follows we discuss a procedure to determine the wind parameters from the CO data. Notice that this procedure is similar to that used by other authors, but we take care to make explicit the assumptions adopted. In general, the determination of the characteristics of the winds of T Tauri stars, such as mass loss rate and

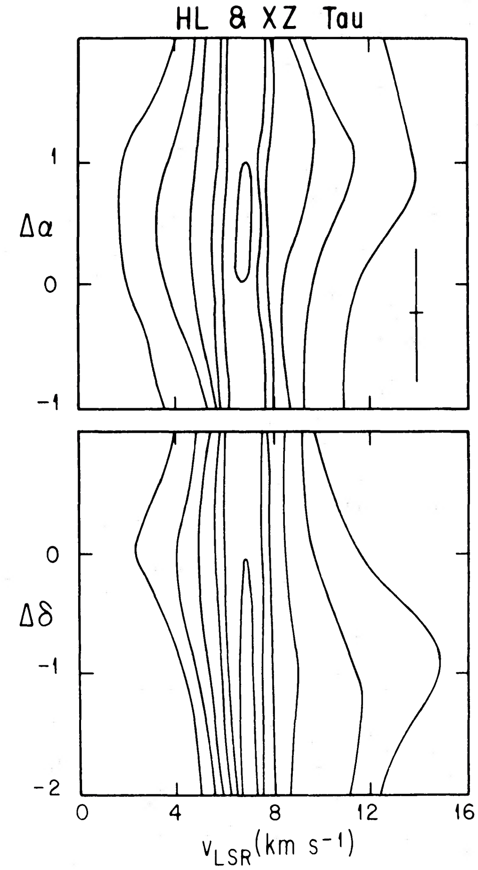

FIG. 3.—Contour maps of the corrected antenna temperature for N-S and E-W cuts along the position of HL Tau. Contour values are 0.5, 1.0, 2.0, 4.0, 6.0, and 8.0 K. Bars indicate angular and velocity resolutions.

velocity, is made from the analysis of one or several infrared, optical, and ultraviolet emission lines from the star's atmosphere, and the results are strongly sensitive to the assumptions in the model used for that analysis (DeCampli 1981). By studying the movement of the molecular material around these stars on the other hand, we have an alternative way of obtaining insight into the properties of the wind, independently of the stellar model. For instance, if we assume that the outflow in the molecular material is produced by the interaction of the stellar wind with the surrounding material, the rates of energy and momentum of the high velocity molecular gas can be regarded as lower limits for the rates carried in the wind, and thus they can impose important restrictions on the parameters of the wind and on the mechanism responsible for it.

In the Appendix we present a formulation to evaluate approximate minimum values for the mass, momentum, kinetic energy and their rates for the material emitting in the wings. The uncertainties on these estimates arise mainly from the lack of knowledge of the physical properties and geometry of the emitting flow. This formulation considers the $J = 1 \rightarrow 0$ rotational transition of the ^{12}CO molecule, and it is based on several simplifying assumptions. First, it is assumed that the line is thermalized and optically thin. Also, the emitting region in the wings is assumed to consist of an isothermal, laminar flow of molecular gas moving in one direction. If we assume the kinetic temperature of the emitting gas to be around 10 K, the calculations of Goldsmith (1972) imply that the $J = 1 \rightarrow 0$ transition of the CO molecule is thermalized for particle densities $\gtrsim 10^3$ cm^{-3}. Since the densities expected in the emitting material are likely to be in this range, our assumption of thermalization is adequate. High-resolution observations of the $J = 2 \rightarrow 1$ and $J = 1 \rightarrow 0$ ^{12}CO lines of several regions of wing emission (see, for instance, Loren *et al.* 1981) indicate that the ratio of antenna temperatures of the $(2 \rightarrow 1)$ to the $(1 \rightarrow 0)$ lines is in general greater than unity in the wings. This is characteristic of optically thin CO and suggests the optically thin case as a reasonable approximation. However, analysis of the ^{13}CO data in some sources suggests moderate optical depths (Edwards and Snell 1982; Bally and Lada 1983). In any case, the optically thin assumption will give lower limits for our estimates.

The formulation given in the Appendix also assumes the flow to be unidimensional. This important assumption is supported by observational and theoretical evidence. Many of the outflows have been found to be bipolar (Rodríguez *et al.* 1982; Bally and Lada 1983), and it can be argued that the apparently isotropic outflows are unresolved bipolars or bipolars observed along the axis of symmetry. For example, in Orion the high-velocity flow was believed to be isotropic until high angular resolution observations (Erickson *et al.* 1982) showed it to be bipolar. To first approximation, bipolar outflows can be described as unidimensional. From the theoretical point of view, laminar and unidimensional flows such as those discussed in Cantó *et al.* (1983; hereafter CTCR) can reproduce the observed CO line profiles and other parameters in outflow sources. Finally, the unidimensional case is the most simplistic assumption we can make about the geometry of the flow. It has to be noticed that this assumption has been used (not always in an explicit way) in similar calculations made by other authors (see, for instance, Bally and Lada 1983). In any event, rough estimates suggest that a different geometry (such as isotropic) gives results within a factor of 2 from the unidimensional case, which is not very significant considering other sources of uncertainty.

Another assumption frequently used regarding the physical state of the emitting material in the wings is that the flow is isothermal. This assumption greatly simplifies the estimation of the kinematical quantities in the flow. There are, however, theoretical indications (CTCR) in the sense that gas emitting in the wings should not be isothermal but that the material moving at higher velocities (with respect to the main line) is hotter. This prediction, on the other hand, has not been tested observationally in an unambiguous way (Loren *et al.* 1981; Levreault 1983). Therefore, in view of the lack of decisive observational evidence we adopt the most simplistic assumption, that is, that the flow is isothermal. The implications of this assumption will be further discussed in CTCR.

Also, the formulation given in the Appendix uses the integration of the observed antenna temperature over the velocity range to estimate the kinematic quantities. Rigorously, we should apply the formulation to every single point observed over the flow region, taking as the size of the region the size of the beam, and then add the values to obtain the estimates for the whole flow region. In this paper, however, we use the spectra in the direction of the exciting star as a representative spectra of the flow region. This assumption is reasonable; for Cep A, Ho, Moran, and Rodríguez (1982) found little variation in the wing slope with position. For the size of the flow we take that estimated from the velocity versus position maps; such a choice is further discussed below. The integrals can easily be estimated following Rodríguez *et al.* (1982) who use the fact that the T_A^* can roughly be fitted by a power law of the radial velocity. In this way the formulae for the kinematical quantities adopt quite simple forms as shown in the Appendix.

The main difference between the formulation given in the Appendix to estimate the kinematic quantities and similar formulations in the literature (see, for instance, Rodríguez *et al.* 1982 and Edwards and Snell 1982) concerns the interpretation of the characteristic time scales. For instance, Edwards and Snell (1982) use the ratio between the spatial extent of the high-velocity gas and the mean velocity of the gas (which actually can be estimated in several different ways) as the characteristic time scale of the flow. However, it is shown in the Appendix that *both* the kinematical quantities and their rates can be estimated directly from the integration of the observed antenna temperatures. Thus, the characteristic times for each quantity can be evaluated by simply dividing the quantity over its rate. This method thus provides a more exact way of calculating parameters. We have to notice here that in this method there is one, in general different, time scale per kinematical quantity. Thus, the most direct and perhaps most meaningful interpretation of these characteristic times is that they represent the time required by the flow to drain, at the present rate, an amount of the related quantity equal to the amount of this quantity which is contained in the flow. Other interpretations of these times, for instance in the sense that they represent dynamical time scales for the flow, are not always correct, since a flow of the kind considered in this work may be maintained even in stationary configurations (see CTCR). Therefore, we prefer to give these times the meaning of drain time scales.

The expressions for the mass, momentum, and kinetic energy and their rates given in equations (A11)–(A16) also involve terms which depend on the orientation (the angle θ) of the emitting flow, assumed to be unidimensional, with respect to the observer's line of sight. In general, the angle θ is not known, and thus the related terms in those expressions are also not known. In equations (A11)–(A13), which give the kinematical quantities, the functions of θ are always greater or equal to unity (see the paragraph below eq. [A17]), and thus the simplest assumption that they equal unity makes our estimates to be strict lower limits. On the other hand, for equations (A14)–(A16), which give the rates of the kinematical quantities, the corresponding functions of θ can be either greater or equal to zero depending on the value of θ. They equal unity for $\theta = 45°$, $51\overset{\circ}{.}8$, and $55\overset{\circ}{.}7$, respectively. Thus, the estimates given by these expressions when assuming the angular terms to be equal to unity are not strict lower limits but only rough estimates. It is important to emphasize that while authors have noted that not accounting for the angle θ makes the estimates for momentum, and kinetic energy to be lower limits, it has not been noted that the projection angle could also make the observationally-determined time scales to be either larger or smaller. Correspondingly, it is not possible to determine if the rates are lower or upper limits.

Let us now apply this formulation to the flows associated with T Tau and HL and XZ Tau. In both cases we adopt a kinetic temperature of 10 K for the emitting flow and place the source at a distance of 160 pc. Also, we use as representative spectra over the whole flow regions those obtained in the direction of the stars. As noted before, this is a reasonable assumption. For T Tau we chose 2.1 and 7.6 km s^{-1} as the minimum and maximum radial velocities, while for HL and XZ Tau we adopted 1.3 and 5.7 km s^{-1}, respectively. The adjusted slopes for the T_A^* versus v_r relationship, on the other hand, were 2.5 and 1.2. We have to emphasize that in our estimates for both sources we only considered the blueshifted wings, since for T Tau the redshifted wing is extremely weak, while for HL and XZ Tau it is likely to be contaminated with emission from the redshifted lobe of L1551 (Snell, Loren and Plambeck 1980). The sizes for the emitting sources follow from Figures 2 and 3; they and our final estimates are shown in Table 3. Regarding the unknown angle θ we face two alternatives, either to choose arbitrarily a value for θ or to impose, inconsistently, that each angular term in the formulae equals unity. We adopted the latter.

If we assume that the outflow in the molecular material is produced by the interaction of the stellar wind from the star with the surrounding material, we can infer that the derived values for the momentum rates are reasonable estimates for the rate of momentum carried in the winds. From these alone we cannot deduce the values of $\dot{M}_\star$ and $V_\star$. We can use, however, Schwartz's (1975) determination for the wind velocity in T Tau (~ 100 km s^{-1}) to estimate $\dot{M}_\star$. For our value for the rate of momentum (Table 3), we obtain $\dot{M}_\star \sim 2.0 \times 10^{-8}$ $M_\odot$ yr^{-1}, in good agreement with Kuhi's (1964) determination, and close to the absolute upper limits set by DeCampli (1981).

In addition, we can use our estimates to discriminate among the several mechanisms which have been proposed for powering the winds around T Tauri stars. We examine here the three most appropriate mechanisms for driving the wind in these stars (DeCampli 1981), namely, radiation pressure, thermal expansion, and deposition of Alfvén waves. We can calculate theoretical values for the rates of energy and momentum carried out by the wind in each case. Table 4 shows the result of such calculation for the rate of momentum. In this table,

TABLE 3

PARAMETERS OF THE OUTFLOWS ASSOCIATED WITH T TAU AND HL AND XZ TAU

Parameter	T Tau	HL and XZ Tau
Angular dimension (arcmin)	~ 4	~ 1
Physical dimension (pc)	0.2	0.05
Mass ($M_\odot$)	0.02	0.001
Rate of mass ($M_\odot$ yr^{-1})	4.7×10^{-7}	6.0×10^{-8}
Mass time scale (yr)	$\sim 5.2 \times 10^4$	1.6×10^4
Momentum ($M_\odot$ km s^{-1})	0.09	0.003
Rate of momentum ($M_\odot$ yr^{-1} km s^{-1})	1.9×10^{-6}	2.1×10^{-7}
Momentum time scale (yr)	$\sim 4.6 \times 10^4$	1.3×10^4
Kinetic energy ($M_\odot$ [km s^{-1}]^2)	0.17	0.005
Rate of kinetic energy ($M_\odot$ yr^{-1} [km s^{-1}]^2)	4.2×10^{-6}	4.0×10^{-7}
Kinetic energy time scale (yr)	$\sim 4.0 \times 10^4$	1.2×10^4

we give the ratio of theoretical to observed rates. Separate values are given for HL Tau and XZ Tau, since it is yet unclear if the wind is produced by either star or both. Luminosities, radii and masses have been taken or estimated from data in Cohen and Kuhi (1979). Even though the energy requirement would be easily fulfilled, the momentum of the wind produced by radiation pressure is small, similar to the case for the outflows powered by OB stars (Kwan and Scoville 1976; Lada and Harvey 1981; Solomon, Huguenin, and Scoville 1981; Rodríguez *et al.* 1982). Thermal expansion by a Parker-type wind would provide plenty of energy and sufficient momentum above our estimates. To estimate coronal temperatures we assumed the radius of the base of the corona to be of the order of the stellar radius (producing upper limits for the quantities in Table 4) and have used $N_e \sim 10^{10}$ cm^{-3} for the base of the corona, consistent with the density of the transition region estimated from ultraviolet data (Cram, Giampapa, and Imhoff 1980) and the theoretical models for the base of this region (Calvet and Basri 1982). Unfortunately, the X-ray luminosity produced by such a hot corona would be of the order of 10^{35} ergs s^{-1}, too far above the observed typical values ($\sim 10^{30}$ ergs s^{-1}). It appears unlikely that extinction in the wind itself could lower the X-ray luminosity by five orders of magnitude (Feigelson and DeCampli 1981; DeCampli 1981). For estimates on the third mechanism, namely energy and momentum deposition by Alfvén waves, we can use the models calculated by DeCampli (1981) and Hartmann, Edwards, and Avrett (1982). For terminal velocities of the order of 200–300 km s^{-1}, the mass loss rate for the resulting wind increases with surface magnetic field strength and stellar radius and decreases with stellar mass in these models. For different values of these parameters, the models predict $\dot{M}_\star$ in the range of 2×10^{-9} to 3×10^{-8} $M_\odot$ yr^{-1}. The corresponding range for the rate of energy and momentum in the wind are, respectively, 6×10^{-3} to 2×10^{-1} $M_\odot$ yr^{-1} (km s^{-1})^2 and 5×10^{-7} to 1.5×10^{-5} $M_\odot$ yr^{-1} km s^{-1}. We note that the radius of the stars where outflows are detected are larger than the values of 2–3 $R_\odot$ assumed in the theoretical calculations, so that the corresponding theoretical $\dot{M}_\star$ should be larger than the values given above. The rates of energy *and* momentum estimated from the radio observations can easily be accounted for by the values predicted by the Alfvén-wave theory. We can conclude that for those stars in which we find evidence for strong winds, the most viable mechanism for powering the wind is energy and momentum deposition by Alfvén waves into the atmosphere of the star. This would require the presence of strong magnetic fields consistently with the high degree of surface activity of the stars, in analogy with the solar case.

According to Hartmann, Edwards, and Avrett (1982), radiative cooling in the wind prevents temperatures larger than 10^5 K from being reached in the atmosphere. Therefore, the existence of a strong cool wind indicates that the atmosphere lacks coronal temperatures. The nondetection of X-ray emission in HL Tau agrees with this conclusion. On the other hand, T Tau has been detected in soft X-rays, although the X-ray luminosity is low indicating that the extent of the high-temperature region is small (Feigelson and DeCampli 1981). The case of T Tau could be interpreted in terms of an inhomogeneous model for the stellar surface, with coexisting zones of different temperature and density. This type of model is similar to that proposed for the "hybrid" stars (Linsky 1980). An alternative explanation would be that the wind detected in T Tau actually comes from its companion, an embedded infrared source which possibly is a low-mass object in a much earlier stage of evolution than T Tau itself (Dyck, Simon, and Zuckerman 1982).

TABLE 4

UPPER LIMITS FOR THE RATIO OF THEORETICAL TO OBSERVED RATES OF MOMENTUM

Star	Radiative	Thermal Expansion	Alfvén Waves
HL Tau ...	0.4	7	2–70
XZ Tau ...	1.0	8	2–70
T Tau......	0.3	4	0.3–8

NOTE.—We give separate values for HL Tau and XZ Tau, since it is yet unclear if the wind is produced by either star or both.

Finally, we should note that although the mass loss rates for T Tauri stars estimated by us (2×10^{-9} to 2×10^{-8} $M_\odot$ yr^{-1}) could be provided by Alfvén waves, other authors (Edwards and Snell 1982) estimate values several times higher (7×10^{-8} to 1×10^{-7} $M_\odot$ yr^{-1}) that cannot be accounted for theoretically. We obtained lower estimates because of the lower H_2/CO ratio adopted and because we did not correct up to account for the fact that the high velocity gas may not fill both the main beam and near error pattern of the antenna. The factor needed to correct for the coupling between antenna and source is poorly known. Assuming that the region of high-velocity gas fills both the main beam and the near error pattern of the antenna when the region is small would lead to underestimating the outflow parameters by a factor of 1.5–2 (Snell and Edwards 1981; Kutner and Ulich 1981). On the other hand, if the region is extended and one assumes that it fills only the main beam, an overestimate of the outflow parameters will result. In any case, we believe that better observational and theoretical restrictions are required to state definite conclusions on the nature of T Tauri winds.

IV. CONCLUSIONS

Our main conclusions are:

1. Gas outflows related to T Tau and HL and XZ Tau have been detected. This result is consistent with the notion that those stars with the most active surfaces, as indicated by their emission-line strength, have powerful winds. We had no detections for the weak-line stars in our program.

2. Among the mechanisms proposed so far for driving the wind in T Tauri stars, the most viable one for the stars detected is that of energy and momentum deposition by Alfvén waves.

3. HL and XZ Tau are located in the molecular cloud L1551 where an independent outflow powered by an infrared source was reported by Snell, Loren, and Plambeck (1980). The detection of a second outflow center in the same cloud certainly suggests that the phenomenon may be very common.

4. Powerful stellar winds are probably present in the pre–main-sequence phase of all stellar types, since the phenomenon of CO outflow has been detected in stars ranging in luminosity from ~ 10–$10^5\ L_\odot$. Observations with higher sensitivity may show the phenomenon to be present around stars of even lower luminosity.

We acknowledge the help of W. Scharlach and J. Weaver during the observing run. This is Contribution 73 of Instituto de Astronomía, UNAM, México.

APPENDIX

MASS, MOMENTUM, KINETIC ENERGY, AND THEIR RATES FOR THE EMITTING MATERIAL IN THE WINGS

In this Appendix we obtain appropriate formulae to evaluate minimum values for the mass, momentum, kinetic energy, and their rates for the emitting material in the wings. For this purpose we will consider the $J = 1 \rightarrow 0$ rotational transition of the ^{12}CO molecule which will be assumed to be thermalized and optically thin. We will assume the emitting region (in the wings) to consist of an unidimensional, laminar flow of molecular gas moving in the $\hat{x}$-direction of an orthogonal frame of reference whose X-Y plane is parallel to the flow. Further, we will regard the flow as isothermal, and we will assume that the other flow variables are functions of z only; a and b will represent the total extent of the flow region in the $\hat{y}$-direction (that is, perpendicular to the flow) and in the $\hat{x}$-direction (that is, along the flow), respectively (see Fig. 4). Then, the total rates of mass, momentum, and kinetic energy perpendicular to the flow direction will approximately be given by

$$\dot{M} \equiv a \int \rho u \, dz\,, \tag{A1}$$

$$\dot{P} \equiv a \int \rho u^2 \, dz\,, \tag{A2}$$

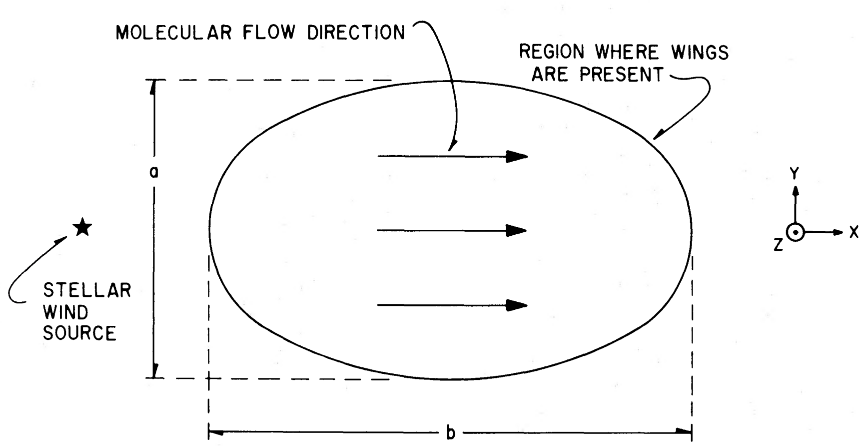

FIG. 4.—A scheme showing the parameters that define the model described in the Appendix

and

$$\dot{E} \equiv a\frac{1}{2}\int \rho u^3\, dz, \tag{A3}$$

where $\rho(z)$ and $u(z)$ are the flow's mass density and velocity, respectively, and the integral extends over the flow region where the emission in the wings are produced. Similarly, the total mass, momentum, and kinetic energy of the material emitting in the wings are roughly given by

$$M \equiv ab\int \rho\, dz, \tag{A4}$$

$$P \equiv ab\int \rho u\, dz, \tag{A5}$$

and

$$E \equiv ab\frac{1}{2}\int \rho u^2\, dz. \tag{A6}$$

In order to evaluate M, P, and E, and their rates from observed quantities, let θ be the angle between the observer's line of sight (contained in the X-Z plane) and the $\hat{z}$-direction. Then the observed radial velocity and depth of the flow region are

$$v_r = u \sin\theta \quad \text{and} \quad s = z/\cos\theta, \tag{A7}$$

respectively. The mass density in terms of the CO particle density, $n(\mathrm{CO})$, is given by

$$\rho = mn(\mathrm{H_2}) = \frac{m}{A(\mathrm{CO})}n(\mathrm{CO}), \tag{A8}$$

where $n(\mathrm{H_2})$ is the particle density of H_2, m is the mass per hydrogen molecule, and $A(\mathrm{CO})$ is the CO abundance with respect to molecular hydrogen. Clearly, the evaluation of equations (A1)–(A6) requires the knowledge of integrals of the form

$$\int \rho u^n\, dz,$$

where n takes values 0–3. With the aid of equations (A7) and (A8), we can write

$$\int \rho u^n\, dz = \frac{m}{A(\mathrm{CO})}\frac{\cos\theta}{\sin^n\theta}\int v_r^n n(\mathrm{CO})\, ds. \tag{A9}$$

On the other hand, using the assumed properties of the flow, in the sense that the line is thermalized and optically thin, then (Rodríguez *et al.* 1982)

$$n(\mathrm{CO})\, ds = BT_A^*\Omega(T)\, dv_r, \tag{A10}$$

where B is a constant ($= 2.3\times 10^{14}$ if dv_r is in km s^{-1}), T_A^* is the corrected antenna temperature and

$$\Omega(T) \equiv \frac{T}{(1-e^{-T^*/T})[J(T)-J(T_B)]}; \qquad J(T) \equiv T^*/(e^{T^*/T}-1),$$

with $T^* \equiv h\nu_{10}/K = 5.53$ K, T the molecular hydrogen kinetic temperature and $T_B = 2.8$ K, the background temperature. Substitution of equation (A10) into equation (A9) gives

$$\int \rho u^n \, dz = \frac{m}{A(\mathrm{CO})} \frac{\cos\theta}{\sin^n\theta} B\Omega(T) \int_{v_{r_{\min}}}^{v_{r_{\max}}} T_A^* v_r^n \, dv_r ,$$

where $v_{r_{\max}}$ and $v_{r_{\min}}$ have the same meaning as in Rodríguez *et al.* (1982), that is, $v_{r_{\min}}$ is the radial velocity where wing emission can no longer be distinguished from the ambient cloud emission, while $v_{r_{\max}}$ is the radial velocity of that point in the wing where it merges with the noise.

If we adopt the following numerical values: $A(\mathrm{CO}) = 10^{-4}$ (which is likely to be a lower limit) and $m \approx 2m_{\mathrm{H}} = 3.34 \times 10^{-24}$ g, then we may write equations (A1)–(A6) as

$$\left(\frac{M}{M_\odot}\right) = 3.1 \times 10^{-3} \cos\theta\, \Omega(T) \left(\frac{D}{\mathrm{kpc}}\right)^2 \left(\frac{\theta_a}{\mathrm{arcmin}}\right)\left(\frac{\theta_b}{\mathrm{arcmin}}\right) I_0 \tag{A11}$$

$$\left(\frac{P}{M_\odot \ \mathrm{km\ s^{-1}}}\right) = 3.1 \times 10^{-3} \frac{\cos\theta}{\sin\theta} \Omega(T) \left(\frac{D}{\mathrm{kpc}}\right)^2 \left(\frac{\theta_a}{\mathrm{arcmin}}\right)\left(\frac{\theta_b}{\mathrm{arcmin}}\right) I_1 \tag{A12}$$

$$\left[\frac{E}{M_\odot (\mathrm{km\ s^{-1}})^2}\right] = 1.6 \times 10^{-3} \frac{\cos\theta}{\sin^2\theta} \Omega(T) \left(\frac{D}{\mathrm{kpc}}\right)^2 \left(\frac{\theta_a}{\mathrm{arcmin}}\right)\left(\frac{\theta_b}{\mathrm{arcmin}}\right) I_2 \tag{A13}$$

and

$$\left(\frac{\dot{M}}{M_\odot \ \mathrm{yr^{-1}}}\right) = 1.1 \times 10^{-8} \frac{\cos\theta}{\sin\theta} \Omega(T) \left(\frac{D}{\mathrm{kpc}}\right)\left(\frac{\theta_a}{\mathrm{arcmin}}\right) I_1 \tag{A14}$$

$$\left[\frac{\dot{P}}{M_\odot \ \mathrm{yr^{-1}} (\mathrm{km\ s^{-1}})}\right] = 1.1 \times 10^{-8} \frac{\cos\theta}{\sin^2\theta} \Omega(T) \left[\frac{D}{\mathrm{kpc}}\right]\left[\frac{\theta_a}{\mathrm{arcmin}}\right] I_2 \tag{A15}$$

$$\left[\frac{\dot{E}}{M_\odot \ \mathrm{yr^{-1}} (\mathrm{km\ s^{-1}})^2}\right] = 5.4 \times 10^{-9} \frac{\cos\theta}{\sin^3\theta} \Omega(T) \left[\frac{D}{\mathrm{kpc}}\right]\left[\frac{\theta_a}{\mathrm{arcmin}}\right] I_3 , \tag{A16}$$

where D is the distance to the source, θ_a and θ_b are the angular sizes of a and b, respectively, and

$$I_n \equiv \int_{v_{r_{\min}}}^{v_{r_{\max}}} T_A^* \left(\frac{v_r}{\mathrm{km\ s^{-1}}}\right)^n \left(\frac{dv_r}{\mathrm{km\ s^{-1}}}\right). \tag{A17}$$

Notice that if the region where wings are present has cylindrical symmetry with respect to its major axis (the x-axis in Fig. 4), the quantity $\theta_b \cos\theta$ in equations (A11) to (A13) represents the *observed* extent of the region in the direction away from the wind source. Thus, since θ_a always coincides with its observed counterpart (whatever the angle θ), the estimation of the total mass in the flow, equation (A11), is independent of θ as it should be.

Following Rodríguez *et al.* (1982) we can further assume that the line wings are described by

$$T_A^* = T_A^*(v_{r_{\min}})(v_r / v_{r_{\min}})^{-\alpha} ,$$

then equation (A17) takes the form

$$I_n = \frac{1}{(n+1-\alpha)} T_A^*(v_{r_{\min}}) \left(\frac{v_{r_{\min}}}{\mathrm{km\ s^{-1}}}\right)^{n+1} \left[\left(\frac{v_{r_{\max}}}{v_{r_{\min}}}\right)^{(n+1-\alpha)} - 1\right], \qquad \alpha \neq n+1$$

or

$$I_n = T_A^*(v_{r_{\min}})\left(\frac{v_{r_{\min}}}{\text{km s}^{-1}}\right)^{n+1} \ln\left(\frac{v_{r_{\max}}}{v_{r_{\min}}}\right), \qquad \alpha = n+1.$$

Frequently it is interesting to compare the values for the rates obtained with the above formulae with the corresponding ones for a stellar wind. To do that, let $\dot{M}_\star$ and $V_\star$ be the mass loss rate and terminal velocity of the wind. Then the rates of mass, momentum and energy (in convenient units) are,

$$\left(\frac{\dot{M}_\star}{M_\odot \text{ yr}^{-1}}\right) = 10^{-7}\left(\frac{\dot{M}_\star}{10^{-7} M_\odot \text{ yr}^{-1}}\right)$$

$$\left[\frac{\dot{M}_\star V_\star}{(M_\odot \text{ yr}^{-1})(\text{km s}^{-1})}\right] = 10^{-5}\left(\frac{\dot{M}_\star}{10^{-7} M_\odot \text{ yr}^{-1}}\right)\left(\frac{V_\star}{100 \text{ km s}^{-1}}\right)$$

$$\left[\frac{1/2\,\dot{M}_\star V_\star^2}{(M_\odot \text{ yr}^{-1})(\text{km s}^{-1})^2}\right] = 5\times 10^{-2}\left(\frac{\dot{M}_\star}{10^{-7} M_\odot \text{ yr}^{-1}}\right)\left(\frac{V_\star}{100 \text{ km s}^{-1}}\right)^2.$$

Finally, characteristic times for each quantity can be estimated by simply dividing the quantity over its rate. For the mass, the characteristic time is

$$\frac{t_M}{\text{yr}} \equiv \frac{M}{\dot{M}} = 2.8\times 10^5 \sin\theta\left(\frac{D}{\text{kpc}}\right)\left(\frac{\theta_b}{\text{arcmin}}\right)\frac{I_0}{I_1},$$

while for momentum and kinetic energy they are

$$\frac{t_P}{\text{yr}} \equiv \frac{P}{\dot{P}} = 2.8\times 10^5 \sin\theta\left(\frac{D}{\text{kpc}}\right)\left(\frac{\theta_b}{\text{arcmin}}\right)\frac{I_1}{I_2}$$

and

$$\frac{t_E}{\text{yr}} \equiv \frac{E}{\dot{E}} = 2.8\times 10^5 \sin\theta\left(\frac{D}{\text{kpc}}\right)\left(\frac{\theta_b}{\text{arcmin}}\right)\frac{I_2}{I_3}.$$

Obviously $t_M \neq t_P \neq t_E$ in general since $I_0/I_1 \neq I_1/I_2 \neq I_2/I_3$ unless u is uniform through the flow region [that is, $u(z) = \text{constant}$]. The most direct (and perhaps most meaningful) interpretation of these characteristic times is that they represent the time required by the flow to drain (at the present rate) an amount of the related quantity equal to the amount of this quantity which is contained in the flow. Other interpretation of these times, in the sense that they represent a dynamical time scale for the flow, is perhaps not always correct since a flow of the kind considered in this Appendix can be maintained even in very long-lived stationary configurations (CTCR). Therefore, we prefer to give these times the meaning of drain time scales.

REFERENCES

Appenzeller, I. 1977, in *IAU Colloquim 42, The Interaction of Variable Stars with Their Environment*, ed. R. Kippenhahn, J. Rahe, and W. Strohmeier *Veröff. Remeis-Sternw. Bamberg*, **11**, No. 121, p. 80.

Bally, J., and Lada, C. J. 1983, *Ap. J.*, **265**, 824.

Beichman, C., and Harris, S. 1981, *Ap. J.*, **245**, 589.

Calvet, N., and Basri, G. S. 1982, in preparation.

Cantó, J. 1978, *Astr. Ap.*, **70**, 111.

_____. 1980, *Astr. Ap.*, **86**, 327.

Cantó, J., and Rodríguez, L. F. 1980, *Ap. J.*, **239**, 982.

Cantó, J., Rodríguez, L. F., Barral, J. F., and Carral, P. 1981, *Ap. J.*, **244**, 102.

Cantó, J., Torrelles, J. M., Calvet, N., and Rodríguez, L. F. 1983, in preparation (CTCR).

Cram, L. E., Giampapa, M. S., and Imhoff, C. L. 1980, *Ap. J.*, **238**, 905.

Cohen, M., and Kuhi, L. V. 1979, *Ap. J. Suppl.*, **41**, 743.

Cohen, M., and Schmidt, G. D. 1983, preprint.

DeCampli, W. M. 1981, *Ap. J.*, **244**, 124.

Dickman, R. L. 1978, *Ap. J. Suppl.*, **37**, 407.

Dyck, H. M., Simon, T., and Zuckerman, B. 1982, *Ap. J. (Letters)*, **255**, L103.

Edwards, S., and Snell, R. L. 1981, *Bull. A.A.S.*, **13**, 540.

_____. 1982, *Ap. J.*, **261**, 151.

Elmegreen, B. 1978, *Moon and Planets*, **19**, 261.

Erickson, N. R. *et al.* 1982, *Ap. J. (Letters)*, **261**, L103.

Feigelson, E., and DeCampli, W. 1981, *Ap. J. (Letters)*, **243**, L89.

Franco, J. 1983, *Ap. J.*, **264**, 508.

Fridlund, C. V., Nordh, H. L., Van Duinen, R. J., Aalders, T. W. G., and Sargent, A. I. 1982, *Astr. Ap.*, in press.
Gahm, G. 1981, *Ap. J. (Letters)*, **242**, L163.
Goldsmith, P. F. 1972, *Ap. J.*, **176**, 597.
Goldsmith, P. F., and Langer, W. D. 1978, *Ap. J.*, **222**, 881.
Hartmann, L., Edwards, S., and Avrett, E. 1982, *Ap. J.*, **261**, 279.
Herbig, G. H. 1966, *Vistas in Astronomy*, **8**, 747.
Herbig, G. H., and Rao, N. K. 1972, *Ap. J.*, **174**, 401.
Herbig, G. H. 1977, *Ap. J.*, **214**, 747.
Ho, P. T. P., Moran, J. M., and Rodríguez, L. F. 1982, *Ap. J.*, **262**, 619.
Knapp, G. R., Kuiper, T. B. H., Knapp, S. L., and Brown, R. L. 1977, *Ap. J.*, **214**, 78.
Kuhi, L. V. 1964, *Ap. J.*, **140**, 1409.
Kutner, M. L., and Ulich, B. L. 1981, *Ap. J.*, **250**, 341.
Kwan, J., and Scoville, N. 1976, *Ap. J. (Letters)*, **210**, L39.
Lada, C. J., and Harvey, P. M. 1981, *Ap. J.*, **245**, 58.
Leung, C. M. 1975, *Ap. J.*, **199**, 340.
Levreault, R. 1983, in preparation.
Linsky, J. L. 1980, in *IAU Colloquim 59, Effects of Mass Loss on Stellar Evolution.*, ed. C. Chiosi and R. Stalio (Dordrecht: Reidel) p. 187.
Loren, R. B., Plambeck, R. L., Davis, J. H., and Snell, R. L. 1981, *Ap. J.*, **245**, 495.
Loren, R. B., and Wooten, H. A. 1978, *Ap. J. (Letters)*, **225**, L81.
Norman, C., and Silk, J. 1980, *Ap. J.*, **238**, 158.
Raymond, J. C. 1979, *Ap. J. Suppl.*, **39**, 1.
Rodríguez, L. F., Carral, P., Ho, P. T. P., and Moran, J. M. 1982, *Ap. J.*, **260**, 635.
Rodríguez, L. F., Ho, P. T. P., and Moran, J. M. 1980, *Ap. J. (Letters)*, **240**, L149.
Rydgren, A. E., Strom, S. E., and Strom, K. M. 1976, *Ap. J. Suppl.*, **30**, 307.
Schwartz, R. D. 1975, *Ap. J.*, **195**, 631.
______. 1978, *Ap. J.*, **223**, 884.
Snell, R. L., and Edwards, S. 1981, *Ap. J.*, **251**, 103.
Snell, R. L., Loren, R. B., and Plambeck, R. L. 1980, *Ap. J. (Letters)*, **239**, L17.
Solomon, P. M., Huguenin, G. R., and Scoville, N. Z. 1981, *Ap. J. (Letters)*, **245**, L19.
Ulich, B. L., and Haas, R. W. 1976, *Ap. J. Suppl.*, **30**, 247.
Walker, M. F. 1956, *Ap. J. Suppl.*, **2**, 365.
______. 1972, *Ap. J.*, **175**, 89.
______. 1978, *Ap. J.*, **224**, 546.
Walter, F. M., and Kuhi, L. V. 1981, *Ap. J.*, **250**, 254.
Zuckerman, B., Kuiper, T. B. H., and Rodríguez Kuiper, E. H. 1976, *Ap. J. (Letters)*, **209**, L137.

N. Calvet: Centro de Investigación de Astronomía, "Francisco J. Duarte," Apartado 264, Mérida, Venezuela

J. Cantó, and L. F. Rodríguez: Instituto de Astronomía, Universidad Nacional Autónoma de México, Apartado Postal 70-264, Ciudad Universitaria, 04510 México, D.F., Mexico